Article

JOURNAL OF THE CHINESE CHEMICAL SOCIETY

Theoretical Study of Substituent Effects on Geometric and Spectroscopic Parameters (IR, ^{13}C, ^{29}Si NMR) and Energy Decomposition Analysis of the Bonding in Molybdenum Silylidyne Complexes $CpMo(CO)_2(\equiv Si\text{-}para\text{-}C_6H_4X)$

Hadis Ghobadi,[a] Reza Ghiasi [b*] and Saeid Jamehbozorgi[c]

[a]*Department of Chemistry, Faculty of Science, Arak branch, Islamic Azad University, Arak, Iran*
[b]*Department of Chemistry, Faculty of Science, East Tehran Branch, Islamic Azad University, Tehran, Iran*
[c]*Department of Chemistry, Faculty of Science, Hamedan Branch, Islamic Azad University, Hamedan, Iran*

(Received: October 28, 2016; Accepted: February 16, 2017; DOI: 10.1002/jccs.201600795)

In this study, we report the substituent effect on the structures, frontier orbital analysis, and spectroscopic properties (IR, ^{13}C, ^{29}Si NMR) in the molybdenum silylidyne complexes $CpMo(CO)_2(\equiv Si\text{-}para\text{-}C_6H_4X)$ (X = H, F, Cl, CN, NO_2, Me, OMe, NH_2, NHMe) using MPW1PW91 quantum chemical calculations. The calculated structural parameters and spectral parameters are compatible with the experimental values in similar complexes. The nature of the chemical bond between the $[Cp(OC)_2Mo]^-$ and $[Si\text{-}para\text{-}C_6H_4X]^+$ fragments was explored with energy decomposition analysis (EDA). The percentage composition in terms of the defined groups of frontier orbitals for $CpMo(CO)_2(\equiv Si\text{-}para\text{-}C_6H_4X)$ complexes was investigated to explore the character of the metal–ligand bonds. The linear correlations between the properties and Hammett constants (σ_p) were illustrated. Natural bond orbital analysis (NBO) was used to illustrate the electronic structure of the complexes.

Keywords: Carbyne complexes; Substituent effect; ^{13}C and ^{29}Si nuclear magnetic resonance chemical shifts; Energy decomposition analysis.

INTRODUCTION

Metal–carbon multiple bonded species supply prolific bases for the investigation of the structure–property–reactivity relationships in organometallic chemistry.[1] The chemical attraction of these complexes is not only due to the primary consideration of bonding and reactivity but also to the value of metal–carbon multiple-bonded species in synthetic organic and polymer chemistry.[2–6]

An extensive range of molybdenum alkylidene complexes have been reported. For example, molybdenum neopentylidyne complexes of the type Mo(C-*t*-Bu)$(OR)_3$ (OR=O-*t*-Bu, $OCMe(CF_3)_2$, $OCH(CF_3)_2$, $OCMe_2(CF_3)$, or O-2,6-*i*-$Pr_2C_6H_3$) have been prepared from Mo(C-*t*-Bu)Cl_3(dme),[7] but development of Mo chemistry was limited by the relatively low yields of the starting material, Mo(C-*t*-Bu)$(CH_2$-*t*-Bu$)_3$. Schrock studied alkyne metathesis by molybdenum and tungsten alkylidyne complexes.[8]

The chemistry of alkylidyne complexes has been a rigorously investigated subject within organometallic science since the discovery of the first transition-metal carbyne complex in 1973.[1] The synthesis, structure, reactivity, and properties of theses complexes have stimulated many studies in the organometallics area.[2–6] They have contributed to numerous catalytic transformations.[9–13] There are silicon analogs of the alkylidyne complexes,[14] and a series of compounds featuring metal–germanium, metal–tin, or metal–lead triple bonds have been obtained by reacting carbonyl metalates.[15,16]

Substituent effect is one of the basic subjects of chemistry, effecting significant changes in the molecular behavior in the presence of the electron-withdrawing groups (EWGs) and electron-releasing groups (ERGs).

In this work, we study the structures of $CpMo(CO)_2(\equiv Si\text{-}para\text{-}C_6H_4X)$ complexes and exemplify the effect of substituents on the structural, electronic, and spectroscopic (IR, and ^{13}C, ^{29}Si NMR) propoerties of these complexes. Furthermore, we use natural bond orbital analysis (NBO) and energy

*Corresponding author. Email: rezaghiasi1353@yahoo.com

decomposition analysis (EDA) in order to gain a deeper insight into the structure and bonding of the complexes. We analyze the nature of Mo≡Si bond in the studied complexes to afford a quantitative differentiation of the Mo≡Si bonds and to reveal the role of the substituent X in the Mo≡Si bond.

RESULTS AND DISCUSSION

Figure 1 presents the molecular structure and atomic numbering of the $CpMo(CO)_2(\equiv Si\text{-}para\text{-}C_6H_4X)$ complexes.

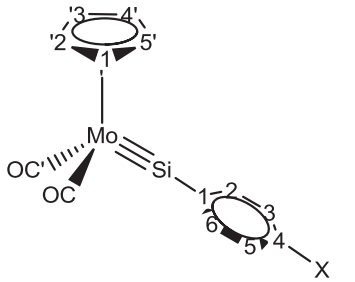

Fig. 1. Molecular structure of $CpMo(CO)_2(\equiv Si\text{-}para\text{-}C_6H_4X)$ complexes (X = H, F, Cl, CN, NO_2, Me, OMe, NH_2, NHMe).

Dipole moments

The dipole moment values of $CpMo(CO)_2(\equiv Si\text{-}para\text{-}C_6H_4X)$ complexes are listed in Table 1. As can be seen from this table, these values increase with decreasing of Hammett constant (σ_p) in the presence of ERGs. But, dipole moment values increase with increasing Hammett constant in the presence of EWGs.

An empirical formula has been proposed relating the constant σ_p in the Hammett equation to the observed dipole moment of a compound (*para*- or *meta*-C_6H_4XY).[17] Similarly, we are interested to find a correlation between the two parameters in the titled complexes. Theoretical studies reveal a good correlation between dipole moments and Hammett constants:

$$\mu = -5.225\ \sigma_p + 3.146;$$
$$R^2 = 0.929,\ X = Me,\ OMe,\ NH_2,\ NHMe$$
$$\mu = 3.385\ \sigma_p + 2.651;$$
$$R^2 = 0.948,\ X = F,\ Cl,\ CN,\ NO_2$$

Isotropic and anisotropic polarizability

The main components of the polarizability tensors as well as the isotropic and anisotropic polarizability values of the complexes are listed in Table 2. These values show that the isotropic and anisotropic polarizability values increase in the presence of ERGs and EWGs. In addition, the polarizabilities of EWG substituents are more than those of ERG substituents. The dipole moments of the molecules are also found to follow the same trend as their polarizabilities.

Structural parameters

Selected bond distances of the $CpMo(CO)_2(\equiv Si\text{-}para\text{-}C_6H_4X)$ complexes have been collected in Table 3. It is well known that the substituent influences both the structure and properties of conjugated organic molecules and metal complexes.[14] The structural data for the optimized structures of the studied complexes are gathered in Table 3. It can be seen that the introduction of the electron-withdrawing substituents results in an increase of the Si–C bond length compared to the corresponding parameters of the unsubstituted molecule. A good correlation is observed between the Si–C bond length and Hammett constants:

$$R(Si-C) = 0.023\ \sigma_p + 1.857;$$
$$R^2 = 0.947;\ X = H,\ Me,\ OMe,\ NH_2,\ NHMe$$
$$R(Si-C) = 0.015\ \sigma_p + 1.856;$$
$$R^2 = 0.999;\ X = F,\ Cl,\ CN,\ NO_2$$

On the other hand, Mo–Si–C_{Ar} bond angles are smaller in the presence of the electron-withdrawing rather than electron-donating substituents. The Mo–C and Mo–Si bond lengths do not show significant variation in the two types of substituents (ERG and EWG).

On the other hand, theoretical results are compatible with experimental values of similar complexes $CpMo(CO)_2(\equiv Si\text{–}Ar)$; Ar = C_6H_3-2,6-$Trip_2$, Trip = 2,4,6-triisopropylphenyl.[14,18] The minor differences are attributed to the fact that the theoretical calculations are based on an isolated molecule in gaseous phase and the experimental results are aimed at the molecule in the solid state. Therefore, the calculated geometric parameters represent a good approximation and they can be used as the foundation to calculate the other parameters of the compound.

Energy decomposition analysis

The Mo≡Si chemical bond in these complexes can be regarded as a donor–acceptor orbital interaction,

Table 1. Absolute energy (hartree), dipole moment (debye), frontier orbitals energies (a.u), and HOMO–LUMO gap (eV) for $CpMo(CO)_2(\equiv Si\text{-}para\text{-}C_6H_4X)$ complexes and Hammett constants of substituents (σ_p)

X	σ_p	E	μ	E(HOMO)	E(LUMO)	Gap
NHMe	−0.70	−1104.3493	7.18	−0.2023	−0.0583	3.917
NH_2	−0.66	−1065.0437	6.13	−0.2044	−0.0609	3.905
OMe	−0.27	−1124.2045	4.81	−0.2091	−0.0663	3.886
Me	−0.17	−1048.9970	3.86	−0.2125	−0.0701	3.876
H	0.00	−1009.6776	3.43	−0.2149	−0.0732	3.854
F	0.06	−1108.9197	3.09	−0.2175	−0.0748	3.883
Cl	0.23	−1469.3073	3.08	−0.2194	−0.0798	3.800
CN	0.66	−1101.9118	5.08	−0.2269	−0.0982	3.503
NO_2	0.78	−1214.1794	5.21	−0.2284	−0.1115	3.180

Table 2. Main components of the polarizability tensor and the isotropic and anisotropic polarizability ($bohr^3$) values for $CpMo(CO)_2(\equiv Si\text{-}para\text{-}C_6H_4X)$ complexes

X	α_{xx}	α_{yy}	α_{zz}	α_{iso}	α_{aniso}
NHMe	414.66	199.46	167.80	260.64	232.65
NH_2	378.68	190.39	158.17	242.41	206.30
OMe	383.22	195.85	164.45	247.84	204.89
Me	367.72	193.06	160.38	240.39	193.09
H	332.64	185.21	150.83	222.89	167.29
F	335.01	184.11	150.92	223.35	169.94
Cl	395.53	195.33	154.74	241.07	212.59
CN	393.75	198.47	156.36	249.84	234.80
NO_2	405.13	189.29	155.12	248.28	218.64

which is schematically illustrated in Figure 2. The fragments $[Si\text{-}para\text{-}C_6H_4X]^+$ have a doubly occupied σ-orbital, which behaves as a donor orbital, and the doubly degenerate empty p(π) orbitals behave as acceptor orbitals. The π interactions in these complexes are tagged as in-plane ($\pi\|$) and out of- plane ($\pi\perp$) π contributions.

We consider the Mo–Si bonding situation in the complexes, which was analyzed with the EDA using the $[Cp(OC)_2Mo]^-$ and $[Si\text{-}para\text{-}C_6H_5]^+$ fragments. The results of EDA reveal that the interaction energies in the studied complexes (−197.2 to −226.7 kcal/mol) are rather high (Table 3). In the $CpMo(CO)_2(\equiv Si\text{-}C_6H_5)$ complex, the total interaction energy between $[Cp(OC)_2Mo]^-$ and $[Si\text{-}para\text{-}C_6H_5]^+$ is −214.40 kcal/mol, the polarization energy of −181.5 kcal/mol stabilized the adduct, while the sum of the electrostatic and exchange energy stabilized the adduct by −32.893 kcal/mol.

The interaction energy values reveal a stronger interaction between $[Cp(OC)_2Mo]^-$ and $[Si\text{-}para\text{-}C_6H_5]^+$ fragments in the presence of EWGs. There is a good linear relationship between the interaction energy values and Hammett constant values:

Table 3. Results of energy decomposition analysis (EDA, in kcal/mol) and the selected structural parameters of $CpMo(CO)_2(\equiv Si\text{-}para\text{-}C_6H_4X)$ complexes (in Å and ° for bond length and bond angle, respectively)

X	ΔE_{int}	ΔE_{polar}	$\Delta E_{els} + \Delta E_{ex}$	Mo–C	Mo–C'	Mo–Si	Si–C	Mo–Si–C_{Ar}
exp	—	—	—	1.9730	1.9680	2.2241	1.8590	173.49
NHMe	−197.22	−173.99	−23.23	1.9509	1.9520	2.2212	1.8401	170.00
NH_2	−200.78	−175.08	−25.70	1.9515	1.9516	2.2206	1.8426	169.59
OMe	−206.17	−178.11	−28.06	1.9526	1.9495	2.2200	1.8490	166.49
Me	−210.39	−180.14	−30.25	1.9510	1.9454	2.2222	1.8546	161.22
H	−214.39	−181.50	−32.89	1.9513	1.9458	2.2217	1.8586	161.06
F	−216.05	−182.37	−33.68	1.9519	1.9454	2.2217	1.8572	160.60
Cl	−216.55	−183.72	−32.83	1.9519	1.9458	2.2218	1.8597	160.26
CN	−224.15	−187.44	−99.95	1.9528	1.9469	2.2217	1.8664	159.50
NO_2	−226.68	−188.18	−38.50	1.9530	1.9473	2.2216	1.8680	159.49

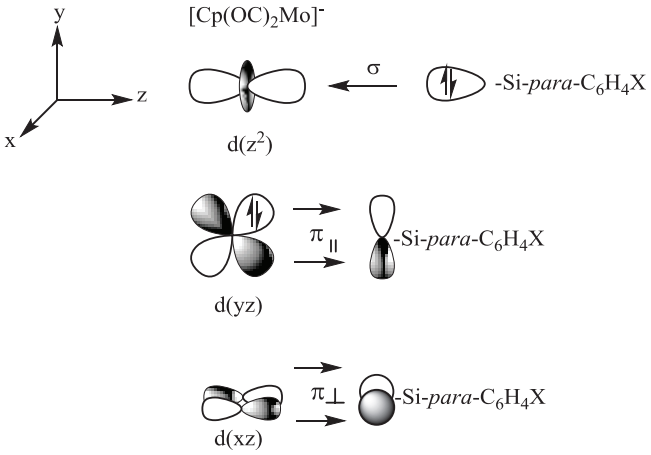

Fig. 2. Schematic representation of the orbital interactions between closed-shell metal fragments $[Cp(OC)_2Mo]^-$ and $[Si\text{-}para\text{-}C_6H_4X]^+$ ligand fragment.

$$\Delta E_{int} = -18.98\ \sigma_p - 212.6;\ R^2 = 0.977$$

On the other hand, the magnitude of ΔE_{polar} increases in the presence of EWGs. There is a good linear relationship between these values and the Hammett constants:

$$-\Delta E_{polar} = 9.549\ \sigma_p + 181.2;\ R^2 = 0.991$$

Also, the magnitude of $\Delta E_{els} + \Delta E_{ex}$ increases in the presence of EWGs.

Vibrational analysis

The wavenumbers of the IR-active symmetric and asymmetric stretching vibrations of C–O groups of $CpMo(CO)_2(\equiv Si\text{-}para\text{-}C_6H_4X)$ complexes are shown in Table 4. It can be seen that the $\upsilon(CO)_{sym}$ and $\upsilon(CO)_{asym}$ values of EWG substituents are higher than those of the ERG substituents. On the other hand, $\upsilon(CO)$ values increase with the Hammett constant of the substituents.

It can be seen that EWG substituent-induced stretching vibrational frequency shifts have a good linear relationship:

$$\upsilon(CO)_{sym} = 8.706\ \sigma_p + 2053.;$$
$$R^2 = 0.996;\ X = H, F, Cl, CN, NO_2$$
$$\upsilon(CO)_{asym} = 10.43\ \sigma_p + 2002.;$$
$$R^2 = 0.988;\ X = H, F, Cl, CN, NO_2$$

Table 4. Wavenumbers of IR-active symmetric and asymmetric stretching vibrations of C–O groups in $CpMo(CO)_2(\equiv Si\text{-}para\text{-}C_6H_4X)$ complexes (in cm^{-1})

X	$\upsilon(CO)_{sym}$	$\upsilon(CO)_{asym}$
Exp[1]	1937.00	1875.00
NHMe	2051.75	2003.79
NH_2	2052.86	2004.90
OMe	2054.13	2005.90
Me	2051.48	2001.19
H	2053.12	2002.97
F	2053.99	2002.82
Cl	2055.02	2004.38
CN	2058.93	2009.22
NO_2	2060.06	2010.80

[1] For $CpMo(CO)_2(\equiv Si\text{–}Ar)$; Ar, C_6H_3-2,6-$Trip_2$ complex; Trip, 2,4,6-triisopropylphenyl.[14]

Molecular orbital analysis

The values of frontier orbital energies and their gap are listed in Table 1. According to the calculation results, frontier orbitals are stabilized in the presence of EWGs and destabilized in the presence of EDGs. There is a good relationship between the frontier orbital energy values and Hammett constants:

$$E(HOMO) = -0.017\ \sigma_p - 0.215;\ R^2 = 0.992$$
$$E(LUMO) = -0.032\ \sigma_p - 0.077;\ R^2 = 0.922$$

The HOMO–LUMO gap, on the other hand, increases in the presence of electron donor groups (EDGs) (and F). On the other hand, this gap decreases in the presence of EWGs. There is a better relationship between the HOMO–LUMO gap and Hammett constants in the presence of EDGs:

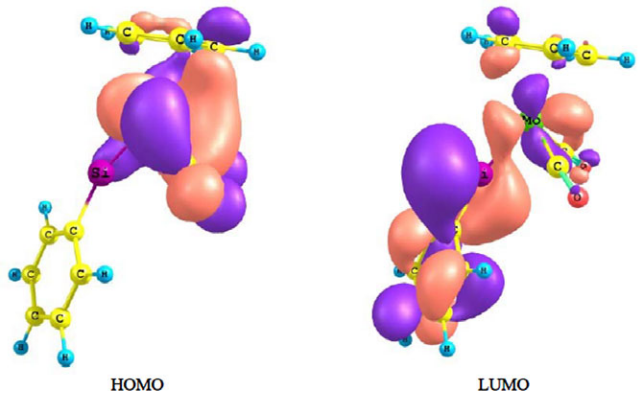

Fig. 3. Frontier orbital distributions of the $CpMo(CO)_2(\equiv Si\text{-}para\text{-}C_6H_5)$ complex.

Table 5. Percentage composition in terms of the defined groups of frontier orbitals for $CpMo(CO)_2(\equiv Si\text{-}para\text{-}C_6H_4X)$ complexes

	HOMO				LUMO			
X	Mo	Silyne	Carbonly	Cp	Mo	Silyne	Carbonly	Cp
NHMe	62	1	28	8	14	78	4	4
NH_2	62	1	28	8	14	78	4	4
OMe	62	2	28	8	15	77	5	4
Me	62	3	27	8	15	77	3	5
H	62	3	27	8	15	77	3	5
F	62	4	26	8	15	76	3	5
Cl	62	3	27	8	14	78	3	5
CN	62	3	27	8	11	84	2	3
NO_2	63	2	27	8	6	90	2	2

$$\text{Gap} = -0.067\ \sigma_p + 3.865;\quad R^2 = 0.951;\ X = \text{Me, OMe, NH}_2\text{, NHMe}$$

$$\text{Gap} = -0.891\ \sigma_p + 3.977;\quad R^2 = 0.915;\ X = \text{F, Cl, CN, NO}_2$$

Therefore, EWGs have the lowest LUMO energy, resulting in the smallest HOMO–LUMO gap for these studied complexes. This behavior arises from an electron-withdrawing inductive effect, which concentrates the electronic density over the substituted region of the complex. On the contrary, the largest HOMO–LUMO gap was established for EDGs due to the electron donating character of the substituent.

These good correlations suggest that EWGs/EDGs influence the frontier orbital energies and the HOMO–LUMO gaps, and these correlations may be employed as a tool to calculate these parameters for other substituents for which σ_p is known.

The frontier orbital distributions of the studied complexes are plotted in Figure 3. The percentage composition in terms of the defined groups of frontier orbitals for $CpMo(CO)_2(\equiv Si\text{-}para\text{-}C_6H_4X)$ complexes is studied to understand the character of the metal–ligand bonds and are listed in Table 5. These values show that the largest contributions of the HOMO arise from Mo, and the contributions of the other ligands are in the order CO > Cp > silyne. On the other hand, the largest contribution of LUMO arises from the silyne group, and the involvements of other fragments are in the order Mo > Cp > CO. Table 5 shows that the contribution of fragments in LUMO depends on the character of X. The contribution of the silyne fragment in the LUMO increases in the presence of EWGs. But, there is no significant variation in the contribution of fragments in the HOMO in the presence of EWGs and EDGs.

^{13}C and ^{29}Si NMR spectra

The ^{13}C and ^{29}Si NMR spectral data for the studied complex are gathered in Table 6. These values exhibit signals for the carbon atom of the carbonyl group at 234.0 ppm and for Si at 325.7 ppm in X = H. ^{29}Si chemical shift values are more in the presence of EDGs than in the presence of EWGs. On the other hand, the ^{13}C chemical shift values of the carbonyl ligand are more in the presence of EDGs than with EWGs.

On the other hand, theoretical results are compatible with experimental values[14] in the complex $CpMo(CO)_2(\equiv Si\text{-}Ar)$; $Ar = C_6H_3\text{-}2,6\text{-}Trip_2$. Therefore, the calculated chemical shifts represent good approximations.

The chemical shift of Si atoms in the studied silylidyne complexes versus σ_p exhibits a linear relationship. The equation is as follows:

$$\delta(^{29}\text{Si}) = -44.19\ \sigma_p + 329.7;\quad R^2 = 0.927$$

The existence of a relation between $\delta(^{29}Si)$ and σ_p is reasonable, since EdGs/EWGs can influence the chemical shift. An electronegative group pulls the electron density out of Si center, resulting in a lower shielding constant.

Again, this correlation may be useful to calculate $\delta(^{29}Si)$ for other substituents for which σ_p is known.

Table 6. ^{1}H and ^{13}C NMR chemical shifts values of $CpMo(CO)_2(\equiv Si\text{-}para\text{-}C_6H_4X)$ complexes (in ppm, with respect to TMS) calculated by CSGT method

X	$C_{carbonyl}$	$C'_{carbonyl}$	C	Si
Exp[1]	231.10	231.10	—	320.10
NHMe	234.28	234.27	134.00	365.96
NH_2	234.20	234.22	134.50	361.72
OMe	234.00	234.18	135.91	348.60
Me	234.08	234.11	139.81	329.47
H	234.01	234.09	142.05	325.67
F	233.90	234.05	138.11	318.06
Cl	233.85	233.94	139.42	314.89
CN	233.94	233.88	144.72	303.97
NO_2	233.97	233.77	147.91	302.29

[1] For $CpMo(CO)_2(\equiv Si\text{–}Ar)$; Ar, C_6H_3-2,6-$Trip_2$ complex; Trip, 2,4,6-triisopropylphenyl.[14]

Natural bond analysis (NBO)

The formal electronic configuration of the Mo atom is $[Kr]4d^5 5s^1$. But the natural electron configuration of the atom in $CpMo(CO)_2(\equiv Si\text{-}C_6H_5)$ complex is

[core]5s(0.38)4d(6.29)5p(0.96)4f(0.01)5d(0.04) 6p(0.01)

On comparing the formal electron configurations with the natural one, the 5s population decreases and 4d population increases. According to the donor–acceptor interactions, the population excess over the formal configuration mainly arises from lone-pair electrons of thre ligands.

The natural electronic configuration of Mo in other $CpMo(CO)_2(\equiv Si\text{-}para\text{-}C_6H_4X)$ complexes are listed in Table 7.

Charge distribution

Figure 4 presents the atomic charge distribution from the natural population analysis (NPA) for the $CpMo(CO)_2(\equiv Si\text{-}C_6H_5)$ complex. Also, the atomic charges of Mo in all complexes are listed in Table 7. These values show that the calculated charges on the Mo atom are considerably less than the formal charge of +2. This is a result of significant charge donation from the ligands. There is a good correlation between the Mo–Si–C_{Ar} angle and charge of Mo:

$$\angle Mo-Si-C_{Ar} = -109.7\, q_{MO} - 18.72;\ R^2 = 0.988$$

When there is more negative charge on Mo, the Mo–Si–C_{Ar} angle increases.

Character of natural hybrid orbital (NHO) in the complexes

Mo–$C_{cabonyl}$ and Mo–C'$_{cabonyl}$ bonds The Mo–$C_{cabonyl}$ and Mo–C'$_{cabonyl}$ bonds of $CpMo(CO)_2(\equiv Si\text{-}C_6H_5)$ are formed by the interaction between $sp^{1.14}d^{4.01}$ and $sp^{1.16}d^{3.90}$ orbitals centered on the Mo ion and an $sp^{0.49}$ orbital on the carbon atom of the carbonyl ligand. The occupancies of the electrons in these bonds are 1.95968 and 1.9610 electrons, respectively. These values of $CpMo(CO)_2(\equiv Si\text{-}para\text{-}C_6H_4X)$ complexes are listed in Table 8.

The polarization coefficients for the formation of the Mo–$C_{cabonyl}$ and Mo–C'$_{cabonyl}$ bonds are 0.6207 and 0.6166 on the Mo, and 0.7840 and 0.7873 on the carbon, respectively. These values show a higher polarization through the carbon atom. This indicates a strong polarization directed toward the C atom. These values for the $CpMo(CO)_2(\equiv Si\text{-}para\text{-}C_6H_4X)$ complexes is listed in Table 8.

Table 7. NBO charges, natural electron configuration of Mo, and Wiberg bond index of Mo–Si bond in $CpMo(CO)_2(\equiv Si\text{-}para\text{-}C_6H_4X)$ complexes

X	*Q*(Mo)	Natural electronic configuration of Mo	WBI(Mo–Si)
NHMe	−1.71693	[core]5s(0.39)4d(6.34)5p(0.99)4f(0.01)5d(0.04)6p(0.01)	1.7332
NH_2	−1.71396	[core]5s(0.39)4d(6.34)5p(0.99)4f(0.01)5d(0.04)6p(0.01)	1.7385
OMe	−1.69212	[core]5s(0.39)4d(6.32)5p(0.98)4f(0.01)5d(0.04)6p(0.01)	1.7426
Me	−1.64546	[core]5s(0.38)4d(6.30)5p(0.96)4f(0.01)5d(0.04)6p(0.01)	1.7270
H	−1.64218	[core]5s(0.38)4d(6.29)5p(0.96)4f(0.01)5d(0.04)6p(0.01)	1.7333
F	−1.63779	[core]5s(0.38)4d(6.29)5p(0.96)4f(0.01)5d(0.04)6p(0.01)	1.7349
Cl	−1.63281	[core]5s(0.38)4d(6.29)5p(0.96)4f(0.01)5d(0.04)6p(0.01)	1.7389
CN	−1.62017	[core]5s(0.38)4d(6.28)5p(0.96)4f(0.01)5d(0.04)6p(0.01)	1.7521
NO_2	−1.61794	[core]5s(0.38)4d(6.27)5p(0.96)4f(0.01)5d(0.04)6p(0.01)	1.7555

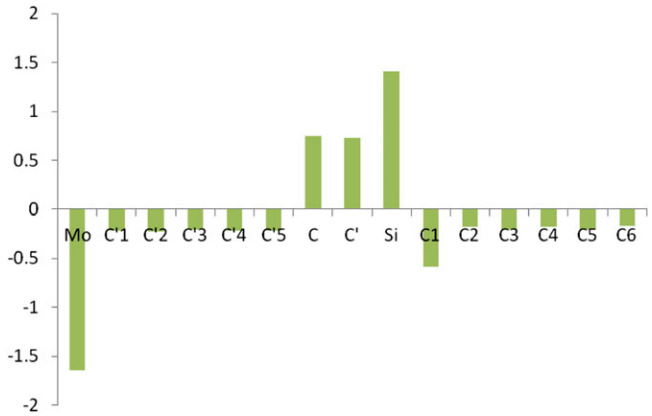

Fig. 4. Atomic charge distribution from the natural population analysis (NPA) for the CpMo $(CO)_2(\equiv Si\text{-}C_6H_5)$ complex.

Mo–Si bond The σ(Mo–Si) bond of $CpMo(CO)_2(\equiv Si\text{-}C_6H_5)$ is formed by the interaction between an $sp^{0.98}d^{1.87}$ orbital centered on the Mo and an $sp^{0.68}$ orbital on the Si atom. The occupancy of the electrons in this bond is 1.90915 electrons. The hybridation orbitals and their occupancies of the σ(Mo-Si) bond of $CpMo(CO)_2(\equiv Si\text{-}para\text{-}C_6H_4X)$ complexes are listed in Table 8 .

The polarization coefficients for the formation of the σ(Mo–Si) bond are 0.6648 on Mo and 0.7288 on Si. These values show a higher polarization through the Si atom. This indicates a strong polarization directed toward the Si atom. These values of $CpMo(CO)_2(\equiv Si\text{-}para\text{-}C_6H_4X)$ complexes are listed in Table 8. NBO results reveal two π(Mo–Si) bonds for $CpMo(CO)_2(\equiv Si\text{-}para\text{-}C_6H_4X)$.

As shown in Table 7, the bond orders of the Mo–Si bond in the studied complexes were obtained using Wiberg bond indices (WBI).[19] This definition of bond order is based on the P matrix and uses the square of the off-diagonal elements of P:

$$B.O_{AB}^{Wiberg} = \sum_{s}^{on\ A} \sum_{t}^{on\ B} P_{st}^2$$

$$P_{st} = \sum_{i}^{occupied} n_i c_{rs} c_{rt} \quad (c_{rs} \text{ and } c_{rt} \text{ the orbital coefficients})$$

The summation is over the molecular orbitals with occupation numbers n_i.

The WBIs of Mo–Si mean obvious bonding interactions, and most values are in the presence of X = NO_2 and CN groups. There is a good linear relationship between WBI(Mo–Si) and Hammett constants in X = H, F, Cl, CN, NO_2 groups:

$$WBI(Mo-Si) = 0.028\ \sigma_p + 1.733; \quad R^2 = 0.998$$

Table 8. Occupancy and calculated natural hybrid (NHOs) of Mo–CO bonds in $CpMo(CO)_2(\equiv Si\text{-}para\text{-}C_6H_4X)$ complexes

X	Occupancy	NBO
NHMe	1.94701	0.7955 (sp 0.49)$_C$ + 0.6059 (sp 1.35d 2.72)$_{Mo}$
	1.94694	0.7950 (sp 0.49)$_{C'}$ + 0.6067 (sp 1.33d 2.72)$_{Mo}$
NH_2	1.94749	0.7944 (sp 0.49)$_C$ + 0.6074 (sp 1.20d 2.71)$_{Mo}$
	1.95702	0.7901 (sp 0.49)$_{C'}$ + 0.6130 (sp 1.15d 3.36)$_{Mo}$
OMe	1.95532	0.7888 (sp 0.49)$_{C'}$ + 0.6146 (sp 1.49d 3.67)$_{Mo}$
	1.95679	0.7902 (sp 0.49)$_C$ + 0.6129 (sp 1.49d 3.66)$_{Mo}$
Me	1.95963	0.7840 (sp0.49)$_{C'}$ + 0.6208 (sp 1.14d 4.00)$_{Mo}$
	1.96112	0.7874 (sp 0.49)$_C$ + 0.6164 (sp 1.16d 3.89)$_{Mo}$
H	1.95968	0.7840 (sp 0.49)$_C$ + 0.6207 (sp 1.14d 4.01)$_{Mo}$
	1.96101	0.7873 (sp 0.49)$_{C'}$ + 0.6166 (sp 1.16d 3.90)$_{Mo}$
F	1.95942	0.7838 (sp 0.49)$_C$ + 0.6210 (sp 1.14d 4.02)$_{Mo}$
	1.96112	0.7876 (sp 0.49)$_{C'}$ + 0.6162 (sp 1.16d 3.90)$_{Mo}$
Cl	1.95948	0.7839 (sp 0.49)$_{C'}$ + 0.6209 (sp 1.14d 4.02)$_{Mo}$
	1.96099	0.7874 (sp 0.49)$_C$ + 0.6165 (sp 1.17d 3.92)$_{Mo}$
CN	1.95412	0.7871 (sp 0.49)$_C$ + 0.6168 (sp 1.15d 3.57)$_{Mo}$
	1.94639	0.7943 (sp 0.49)$_{C'}$ + 0.6075 (sp 1.25d 2.82)$_{Mo}$
NO_2	1.95961	0.7843 (sp 0.49)$_C$ + 0.6203 (sp 1.16d 4.04)$_{Mo}$
	1.96077	0.7870 (sp 0.49)$_{C'}$ + 0.6170 (sp 1.18d 3.97)$_{Mo}$

COMPUTATIONAL METHODS

All calculations were performed with the Gaussian 09 suite program.[20] The calculations of systems contain main groups elements described by the standard 6-311G(d,p) basis set.[21–24] For Mo element, standard Def2-TZVPPD basis set was used[25] and Mo was described by the effective core potential (ECP) using the Def2-TZVPPD basis set.[26] Geometry optimization was carried out with the modified Perdew–Wang exchange and correlation (MPW1PW91).[27] A vibrational analysis was performed at each stationary point found, confirming its identity as an energy minimum.

Population analysis was also performed by the NBO method[28] using the NBO program.

The percentage contributions of atomic orbitals in the HOMO and LUMO (frontier orbitals) were found by the GaussSum 2.2 software package.[29]

Chemical shift values were calculated using the continuous set of gauge transformations (CSGT) method at the same method and basis sets of optimization.[30–32]

The bonding interactions between the $[Cp(OC)_2Mo]^-$ and $[Si\text{-}para\text{-}C_6H_5]^+$ fragments were analyzed by means of the EDA implemented in the Multiwfn3.3.5. package.[33] In this method, the instantaneous interaction energy (E_{int}) between the two fragments can be divided into three main components:

$$\Delta E_{int} = \Delta E_{polar} + \Delta E_{els} + \Delta E_{Ex}$$

E_{polar} is electron density polarization term (also called as the induction term)

$= E$ (SCF last) $- E$ (SCF first)

E_{els} is the electrostatic interaction term, and E_{Ex} is the exchange repulsion term.

CONCLUSIONS

Theoretical calculations on the molybdenum silylidyne complexes $CpMo(CO)_2(\equiv Si\text{-}para\text{-}C_6H_4X)$ indicated that dipole moments increase with decreasing Hammett constant (σ_p) in the presence of ERGs. EDA analysis revealed that the interaction energies are quite strong in the all the studied complexes. Molecular orbital analysis showed the contribution of silylidyne fragment in LUMO increases in the presence of withdrawing groups, and there are no important changes on the contribution of fragments in HOMO in the presence of EWGs and EDGs. Vibrational analysis revealed the $\upsilon(CO)_{sym}$ and $\upsilon(CO)_{asym}$ values of EWG substituents are more than ERG substituents. There is good dependence of the chemical shift values of Si atoms in the studied silylidyne complexes versus σ_p. NBO analysis showed higher polarization through the Si and C atoms in Mo–Si and M–CO bonds, respectively.

REFERENCES

1. E. O. Fischer, G. Kreis, C. G. Kreiter, J. Müller, G. Huttner, H. Lorenz, *Angew. Chem. Int. Ed.* **1973**, *12*, 564.
2. R. E. D. Re, M. D. Hopkins, *Coord. Chem. Rev.* **2005**, *249*, 1396.
3. J. W. Herndon, *Coord. Chem. Rev.* **2003**, *243*, 3.
4. D. J. Mindiola, *Acc. Chem. Res.* **2006**, *39*, 813.
5. R. L. Cordiner, P. A. Gugger, A. F. Hill, A. C. Willis, *Organometallics* **2009**, *28*, 6632.
6. L. Colebatch, A. F. Hill, R. Shang, A. C. Willis, *Organometallics* **2010**, *29*, 6482.
7. L. G. McCullough, R. R. Schrock, J. C. Dewan, J. S. Murdzek, *J. Am. Chem. Soc.* **1985**, *107*, 5987.
8. R. R. Schrock, *Chem. Commun.* **2013**, *49*, 5529.
9. F. O. Fischer, *Adv. Organomet. Chem.* **1976**, *14*, 1.
10. F. G. A. Stone, *Angew. Chem. Int. Ed. Engl.* **1984**, *23*, 89.
11. R. R. Schrock, *Acc. Chem. Res.* **1986**, *19*, 342.
12. H. P. Kim, R. J. Angelici, *Adv. Organomet. Chem.* **1987**, *27*, 51.
13. H. Fischer, P. Hofmann, F. R. Kreißl, R. R. Schrock, U. Schubert, K. Weiss, *Carbyne Complexes*, VCH, Weinheim, **1988**.
14. A. C. Filippou, O. Chernov, K. W. Stumpf, G. Schnakenburg, *Angew. Chem. Int. Ed.* **2010**, *49*, 3296.
15. R. S. Simons, P. P. Power, *J. Am. Chem. Soc.* **1996**, *118*, 11966.
16. L. Pu, B. Twamley, S. T. Haubrich, M. M. Olmstead, B. V. Mork, R. S. Simons, P. P. Power, *J. Am. Chem. Soc.* **2000**, *122*, 650.
17. L. K. H. V. Beek, *Recl. Trav. Chim. Pays-Bas* **1957**, *76*, 729.
18. C. W. Landorf, M. M. Haley, *Angew. Chem. Int. Ed.* **2006**, *45*, 3914.
19. K. B. Wiberg, *Tetrahedron* **1968**, *24*, 1083.
20. M. J. Frisch, G. W. Trucks, H. B. Schlegel, G. E. Scuseria, M. A. Robb, J. R. Cheeseman, G. Scalman, V. Barone, B. Mennucci, G. A. Petersson, H. Nakatsuji, M. Caricato, X. Li, H. P. Hratchian, A. F. Izmaylov, J. Bloino, G. Zheng, J. L. Sonnenberg, M. Hada, M. Ehara, K. Toyota, R. Fukuda, J. Hasegawa, M. Ishida, T. Nakajima, Y. Honda, O. Kitao, H. Nakai, T. Vreven,

J. A. Montgomery Jr.. , J. E. Peralta, F. Ogliaro, M. Bearpark, J. J. Heyd, E. Brothers, K. N. Kudin, V. N. Staroverov, R. Kobayashi, J. Normand, K. Raghavachari, A. Rendell, J. C. Burant, S. S. Iyengar, J. Tomasi, M. Cossi, N. Rega, J. M. Millam, M. Klene, J. E. Knox, J. B. Cross, V. Bakken, C. Adamo, J. Jaramillo, R. Gomperts, R. E. Stratmann, O. Yazyev, A. J. Austin, R. Cammi, C. Pomelli, J. W. Ochterski, R. L. Martin, K. Morokuma, V. G. Zakrzewski, G. A. Voth, P. Salvador, J. J. Dannenberg, S. Dapprich, A. D. Daniels, O. Farkas, J. B. Foresman, J. V. Ortiz, J. Cioslowski, D. J. Fox, *Revision A.02 ed*, Gaussian, Inc, Wallingford, CT, **2009**.

21. P. J. Hay, *J. Chem. Phys.* **1977**, *66*, 4377.
22. R. Krishnan, J. S. Binkley, R. Seeger, J. A. Pople, *J. Chem. Phys.* **1980**, *72*, 650.
23. A. D. McLean, G. S. Chandler, *J. Chem. Phys.* **1980**, *72*, 5639.
24. A. J. H. Wachters, *J. Chem. Phys.* **1970**, *52*, 1033.
25. D. Rappoport, F. Furche, *J. Chem. Phys.* **2010**, *133*, 134105.
26. D. Andrae, U. Haeussermann, M. Dolg, H. Stoll, H. Preuss, *Theor. Chim. Acta* **1990**, *77*, 123.
27. C. Adamo, V. Barone, *J. Chem. Phys.* **1998**, *108*, 664.
28. A. E. Reed, L. A. Curtiss, F. Weinhold, *Chem. Rev.* **1988**, *88*, 899.
29. N. M. O'Boyle, A. L. Tenderholt, K. M. Langer, *J. Comput. Chem.* **2008**, *29*, 839.
30. T. A. Keith, R. F. W. Bader, *Chem. Phys. Lett.* **1992**, *194*, 1.
31. T. A. Keith, R. F. W. Bader, *Chem. Phys. Lett.* **1993**, *210*, 223.
32. J. R. Cheeseman, G. W. Trucks, T. A. Keith, M. J. Frisch, *J. Chem. Phys.* **1996**, *104*, 5497.
33. T. Lu, F. Chen, *J. Mol. Graph. Model.* **2012**, *38*, 314.

